In vivo Diagnosis of Epidermal Growth Factor Receptor Expression using Molecular Imaging with a Cocktail of Optically Labeled Monoclonal Antibodies

Tristan Barrett,[1] Yoshinori Koyama,[1] Yukihiro Hama,[1] Gregory Ravizzini,[1] In Soo Shin,[2] Beom-Su Jang,[2] Chang H. Paik,[2] Yasuteru Urano,[3] Peter L. Choyke,[1] and Hisataka Kobayashi[1]

Abstract

Purpose: Epidermal growth factor receptors (EGFR) play an important role in tumorigenesis and, therefore, have become targets for new molecular therapies. Here, we use a "cocktail" of optically labeled monoclonal antibodies directed against EGFR-1 (HER1) and EGFR-2 (HER2) to distinguish tumors by their cell surface expression profiles.

Experimental Design: *In vivo* imaging experiments were done in tumor-bearing mice following s.c. injection of A431 (overexpressing HER1), NIH3T3/HER2+ (overexpressing HER2), and Balb3T3/DsRed (non-expression control) cell lines. After tumor establishment, a cocktail of optically labeled antibodies: Cy5.5-labeled cetuximab (anti-HER1) and Cy7-labeled trastuzumab (anti-HER2) was i.v. injected. *In vivo* and *ex vivo* fluorescence imaging was done. For comparison with radionuclide imaging, experiments were undertaken using ^{111}Indium-labeled antibodies. Additionally, a "blinded" diagnostic study was done for mice bearing one tumor type.

Results: *In vivo* spectral fluorescent molecular imaging of 14 mice with three tumor types clearly differentiated tumors using the cocktail of optically labeled antibodies both *in vivo* and *ex vivo*. Twenty-four hours after injection, A431 and NIH3T3/HER2+ tumors were detected distinctly by their peak on Cy5.5 and Cy7 spectral images, respectively; radionuclide imaging was unable to clearly distinguish tumors at this time point. In blinded single tumor experiments, investigators were able to correctly diagnose a total of 40 tumors.

Conclusion: An *in vivo* imaging technique using an antibody cocktail simultaneously differentiated two tumors expressing distinct EGFRs and enabled an accurate characterization of each subtype.

Molecular imaging probes typically contain three components: a targeting moiety, a linker, and an imaging beacon. The linker is attached to the targeting moiety in a manner that does not disturb its binding affinity. Various targeting moieties have been employed for molecular imaging including peptides, antibodies, and antibody fragments. Imaging beacons include magnetic resonance contrast agents such as gadolinium (III) or iron, radionuclide or positron emitters, ultrasound microbubbles, and optically fluorescent probes. Several molecular imaging agents have been designed to carry dual or triple probes in which a single targeting moiety is linked to two or more imaging beacons allowing multiple imaging modalities to be done. The use of multiple targeting moieties is less common but could be useful given the heterogeneous nature of tumor cell surface expression. Tumors show genomic and proteomic diversity, leading to expression profiles that vary widely both within a single lesion and among many lesions. This diversity of expression can currently only be assessed by invasively obtaining tissue samples from multiple sites, followed by time-consuming genetic typing and immunohistochemistry. The ability to identify specific cell expression profiles *in vivo* and in real-time opens the opportunity for more accurate sampling of tumor tissue than is now possible with visible light alone.

The epidermal growth factor receptor (EGFR) family consists of four types of ErbB receptor tyrosine kinases. The four members include HER1 (also known as EGFR-1 or ErbB1), HER2 (EGFR-2, c-neu, ErbB2), HER3 (ErbB3), and HER4 (ErbB4; refs. 1, 2). Each receptor consists of a tyrosine kinase, a glycosylated ligand-binding domain, and a transmembrane anchor. All of these receptors have been shown to be key regulators of normal cellular signaling and development (3). These receptors play an important role in carcinogenesis; overexpression of one or more EGFRs has been shown in a number of malignancies, including ovarian, breast, non–small

Authors' Affiliations: [1]Molecular Imaging Program, Center for Cancer Research, National Cancer Institute, and [2]Nuclear Medicine Department, Warren Magnuson Clinical Center, NIH, Bethesda, Maryland; and [3]Graduate School of Pharmaceutical Sciences, The University of Tokyo, Tokyo, Japan

Received 5/8/07; revised 7/23/07; accepted 8/21/07.

Grant support: Intramural Research Program of the NIH, National Cancer Institute, Center for Cancer Research.

The costs of publication of this article were defrayed in part by the payment of page charges. This article must therefore be hereby marked *advertisement* in accordance with 18 U.S.C. Section 1734 solely to indicate this fact.

Note: Supplementary data for this article are available at Clinical Cancer Research Online (http://clincancerres.aacrjournals.org/).

T. Barrett and Y. Koyama contributed equally to this work.

Requests for reprints: Hisataka Kobayashi, Molecular Imaging Program, Center for Cancer Research, National Cancer Institute, NIH, Building 10, Room 1B40, Bethesda, MD 20892-1088. Phone: 301-435-4086; Fax: 301-402-3191; E-mail: kobayash@mail.nih.gov.

doi:10.1158/1078-0432.CCR-07-1119

cell lung cancer, and squamous cell carcinomas. Furthermore, high levels of expression often correlate with a poor prognosis (4–6). In addition, these receptors have recently been found to be excellent epitopes for molecularly targeted cancer therapy. Therapeutic monoclonal antibodies targeting several of these receptors have recently been approved by the Food and Drug Administration (FDA): cetuximab—a chimeric human-murine antibody specific for HER1 receptors, and trastuzumab—a humanized anti-HER2 antibody are both in clinical use. However, the diagnostic potential of these agents has not yet been fully realized. It should be possible to use these agents, at considerably lower doses, as targeting moieties for imaging agents to better characterize the nature of tumor *in vivo*.

Optical imaging is ideally suited to multitargeted *in vivo* molecular imaging, offering a technique with high sensitivity and specificity, with excellent temporal and spatial resolution, but without exposure to ionizing radiation. In addition, more than one wavelength of light can be resolved using spectral imaging, thus, it is possible to simultaneously discern two or more optical probes each labeled with a different fluorophore (1, 7). If each fluorophore is conjugated to a different targeting agent (e.g., antibody), then it should be possible to resolve two or more populations of cells expressing these antigens. The main drawback of optical imaging is its limited depth of tissue penetration. *In vivo* optical imaging typically employs imaging in the near-IR (NIR) range of the optical spectra (650-900 nm). This is because hemoglobin, muscle, and fat are least efficient in absorbing light in the NIR range, allowing deeper tissue penetration of photons (7). Further advances in imaging technology, nanotechnology, and in the mathematical models used to map photon pathways may enable detection from deeper within tissues. However, at present, optical imaging is mainly limited to animal models, or surface applications in humans.

Here, we present a model in which two monoclonal antibodies (cetuximab and trastuzumab) were labeled with NIR optical probes and were then injected into mice with tumors expressing distinct EGFR subtypes in order to determine whether such a "cocktail" of molecular imaging agents could distinguish different cell types *in vivo*.

Materials and Methods

Tumor cells

Two established cell lines were used: A431—a human epidermoid carcinoma cell line overexpressing the HER1 receptor, but minimally expressing the HER2 receptor, and NIH3T3—murine fibroblast–like cells. NIH3T3 cells do not express HER1 or HER2 receptors. The NIH3T3 cells were transfected with HER2 genes (3T3/HER2+), in order to overexpresses HER2 receptors (8). A431 cell lines were cultured in DMEM (Life Technologies), containing 10% fetal bovine serum (Life Technologies). 3T3/HER2+ cells were grown in RPMI 1640 (Life Technologies) containing 10% fetal bovine serum, 0.03% L-glutamine at 37°C, 100 units/mL of penicillin, and 100 μg/mL of streptomycin in 5% CO_2. Balb3T3 cell lines (American Type Culture Collection) were also employed as a negative control. These control cells did not express HER1 or HER2 receptors and were transformed by murine sarcoma virus and transfected with red fluorescence protein genes (Balb3T3/DsRed).

Transfection of red fluorescence protein (DsRed2) to Balb3T3 cells for validation

The red fluorescence protein, DsRed2-expressing plasmid, was purchased from Clontech Laboratories, Inc. The plasmid was transfected into the Balb3T3 cells in order to validate the results with targeted fluorophores (see below). The transfection of red fluorescence protein was done with an electroporation method using Gene Plus II (Bio-Rad Laboratories). Briefly, 3 μg of DsRed2-expressing plasmid was mixed with 2 million Balb3T3 cells in 400 μL of the cell culture medium (RPMI 1640 with 10% fetal bovine serum). The cell suspension was then placed in a pulse cuvette with a 4-mm gap (Bio-Rad Laboratories) and 250-V pulses were delivered after 950 cycles. The Balb3T3/DsRed cell was then cloned with the limited dilution culture method.

Synthesis of antibody-conjugated NIR fluorescence dyes

Antibodies and fluorescent dyes. Erbitux, a FDA-approved chimeric human murine antibody specific for HER1 receptors, generically known as cetuximab, was purchased from Bristol-Myers Squibb Company. Herceptin, a FDA-approved humanized anti-human EGFR type 2 (HER2) antibody, generically known as trastuzumab, which has a complimentary determination region against HER2 grafted on a human IgG_1 framework, was purchased from Genentech, Inc. Rhodamine green (RhodG) was purchased from Invitrogen Corporation. Cy5.5 NHS ester and Cy7 NHS ester were purchased from GE Healthcare.

Conjugation process. At room temperature, 500 μg (3.3 nmol) of cetuximab or trastuzumab in Na_2HPO_4 was incubated with 20 nmol of RhodG, 40 nmol of Cy5.5 NHS ester, or 30 nmol of Cy7 NHS ester dissolved in 5 mmol/L of DMSO, respectively, at pH 8.5 for 15 min at room temperature. The mixture was purified with a Sephadex G50 column (PD-10; GE Healthcare). Cetuximab-conjugated RhodG, trastuzumab-conjugated RhodG, cetuximab-conjugated Cy5.5, and trastuzumab-conjugated Cy7 samples (cetuximab-RhodG, trastuzumab-RhodG, cetuximab-Cy5.5, and trastuzumab-Cy7, respectively) were kept at 4°C in the refrigerator as stock solutions. The protein concentration of cetuximab-RhodG, trastuzumab-RhodG, cetuximab-Cy5.5, and trastuzumab-Cy7 samples were determined with Coomassie Plus protein assay kit (Pierce Biotechnology) by measuring the absorption at 595 nm with a UV-Vis system (8453 Value UV-Visible Value System, Agilent Technologies) using standard solutions of known concentrations of cetuximab or trastuzumab (100, 200, and 400 μg/mL). Then, the concentration of RhodG, Cy5.5, or Cy7 was measured by the absorption at 503, 675, and 747 nm, respectively, with the UV-Vis system to confirm the number of fluorophore molecules conjugated with each cetuximab or trastuzumab molecule. The number of fluorophore molecules per cetuximab or trastuzumab was adjusted to ~2.

Radiolabeling of antibodies

Both antibodies were concentrated to ~5 mg/mL and diafiltrated against 0.1 mol/L of PB at pH 9 with Centricon YM-50 (Millipore Corporation). Antibodies were reacted with a 20-fold molar excess of [(R)-2-amino-3-(4-isothiocyanatophenyl)propyl]-trans-(S,S)-cyclohexane-1,2-diamine-pentaacetic acid (CHX-A″), which was purchased from Macrocyclics as previously described (9, 10). Carrier-free $^{111}InCl_3$ was purchased from Perkin-Elmer. Both antibodies conjugated with CHX-A″ were reacted with ^{111}In in 0.2 mol/L of sodium acetate buffer at pH 4.2 for 1 h at room temperature, as previously described (9, 11). The specific activities of the radiolabeled antibodies were 5.6 mCi/mg for cetuximab and 6.0 mCi/mg for trastuzumab. Purity was >98% as determined by instant TLC (GelmanSciences), developed with a solvent mixture containing 3:2:1 methanol/10% ammonium acetate in water/0.5 mol/L citric acid and size exclusion high-performance liquid chromatography using a TSK G3000SWxL column [0.07 mol/L PBS, 0.1 mol/L KCl (pH 6.8), 1 mL/min; Tosoh Bioscience LLC]. On instant TLC, ^{111}In-labeled antibodies remains at the origin, whereas free ^{111}In moves to the solvent front as ^{111}In citrate. The retention time of radiolabeled antibodies is 8.9 min on the size exclusion high-performance liquid chromatography.

Flow cytometry study

One-color flow cytometry was done for the assessment of the specificity of cetuximab-RhodG against A431 cells and trastuzumab-RhodG

against 3T3/HER2+ cells because flow cytometry is not efficient in the NIR range. 3T3/HER2+ cells (1×10^4) were plated on a 12-chamber well and incubated for 16 h. Cetuximab-RhodG or trastuzumab-RhodG was added to the medium (1 μg/mL) and the cells were incubated for 3 h. Three hours after incubation, flow cytometry was done. The argon ion 488 nm laser was employed for excitation. Signals from cells were collected using a 530/30 nm band-pass filter. Cells were analyzed in a FACScan cytometer (Becton Dickinson) and all data were analyzed using CellQuest software (Becton Dickinson). The fluorescence capability of each fluorophore was referred to as the mean fluorescence index.

Fluorescence microscopy

Two sets of A431 and 3T3/HER2+ cells (each 1×10^4) were plated on a cover glass–bottomed culture well and incubated for 16 h. Either cetuximab-Cy5.5 or trastuzumab-Cy7 was added to each of the four cultured media (30 μg/mL). The cells were incubated and removed at the following time points: 1, 4, 8, 24, and 48 h. Following removal, cells were washed once with PBS and fluorescence microscopy was immediately done using an Olympus BX61 microscope (Olympus America, Inc.) equipped with the two following filter settings: excitation wavelength 590 to 650 nm, emission wavelength 662.5 to 737.5 nm for Cy5.5 spectra range, and excitation wavelength 672.5 to 747.5 nm, and emission wavelength 765 to 855 nm for Cy7 spectra range. Transmitted light differential interference contrast images were also acquired. A431 cells incubated with trastuzumab-Cy7 and 3T3/HER2+ cells incubated with cetuximab-Cy5.5 served as "crossover" negative controls for the fluorescence microscopy experiments.

Immunoreactivity and Scatchard plot analysis

The immunoreactivity of the radiolabeled cetuximab or trastuzumab was determined using a previously described cell-binding assay (12). In brief, aliquots of ^{111}In-labeled cetuximab or trastuzumab (3 ng/100 μL) were incubated for 1 h at 4°C with 2×10^6 A431 or 3T3/HER2+ or Balb3T3/DsRed cells. The cell-bound radioactivity was separated by centrifugation and counted in a gamma-counter. Nonspecific binding to the cells was examined under conditions of antibody excess (20 μg of nonradiolabeled antibodies). The specific binding was obtained by subtracting the nonspecific cell-bound radioactivity from the total cell-bound radioactivity.

In order to validate the number of receptors in each cell, Scatchard plot analyses were done as previously described (13). In brief, serial dilutions of ^{111}In-labeled cetuximab or trastuzumab (10, 20, 50, 100, and 200 ng/100 μL) were incubated for 1 h at 4°C with 2×10^5 A431 or 3T3/HER2+ cells suspended in 100 μL of PBS. The specific binding was obtained by subtracting the nonspecific cell-bound radioactivity from the total cell-bound radioactivity as described above, and the receptor number on each cell was calculated.

Animal model

All procedures were carried out in compliance with the Guide for the Care and Use of Laboratory Animal Resources (1996), National Research Council, and approved by the local Animal Care and Use Committee. Two each of A431, 3T3/HER2+ and Balb3T3/DsRed tumors were established. For each cell line, 2 million (200 μL) cells, suspended in PBS, were injected s.c. onto the back of the mice, following i.p. administration of ketamine (90 mg/kg; Ketaset, Aveco, Inc.) with xylazine (9 mg/kg; AnaSed, Lloyd, Inc.) as a general anesthetic. A431 cells were implanted on the left shoulder and right hip, 3T3/HER2+ cells on the right shoulder and left hip, and Balb3T3/DsRed cells on bilateral flank regions (Supplemental Fig. S1). Tumors were monitored for growth and imaging was undertaken when tumors reached an appropriate size (10-14 days after implantation).

In vivo spectral fluorescence imaging study

Initial "baseline" experiments using A431 and 3T3/HER2+ tumors were done to determine proof of principle, tumor growth rates, antibody dosage, and time of imaging post-antibody administration. Fourteen female nude mice (National Cancer Institute Animal Production Facility) were implanted with tumors (as described above). A 200 μL mixture containing 50 μL (concentration of 1 μg/μL) of each antibody-optical agent conjugate and 100 μL of PBS was prepared. The antibody cocktail was injected i.v. via the mouse tail vein 24 h prior to optical imaging. Prior to imaging, mice were anesthetized with i.p. administered 10% pentobarbital sodium (nembutal, Abbott Laboratories) with 0.1% scopolamine butylbromide (buscopan injection, Nippon Boehringer Ingelheim, Co.). Spectral fluorescence images were obtained using the Maestro In-Vivo Imaging System (CRi, Inc.). For a red light filter, a band-pass filter from 615 to 665 nm and a long-pass filter over 700 nm were used for excitation and emission light, respectively. The tunable filter was automatically stepped in 10-nm increments from 650 to 950 nm, whereas the camera captured images at each wavelength interval with constant exposure. Spectral fluorescence images based on autofluorescence, Cy5.5, and Cy7 spectra were obtained. Spectral libraries for Cy5.5 and Cy7 were imported and the respective spectra unmixed (see Fig. 1 for schema), using commercial software (Maestro software, CRi, Inc.). Specifically, blood pool images from non–tumor-containing regions were unmixed from tumor-containing regions to reduce background contamination from the unbound optically labeled antibodies. Mice were sacrificed with carbon dioxide immediately after completion of imaging. Surgery was then done to resect the tumors and enable *ex vivo* optical imaging, using the same Maestro settings.

Semiquantitative biodistribution and tumor accumulation analysis using scintigraphy obtained with ^{111}In-labeled antibodies

Indium (^{111}In) labeled antibody conjugates were injected into mice bearing multiple tumors to monitor antibody biodistribution. Four mice were injected i.v. with 280 μCi/50 μg of ^{111}In-cetuximab, and four mice with 300 μCi/50 μg ^{111}In-trastuzumab. Serial scintigraphy was obtained at 1, 2, and 4 days after injection of each radiolabeled antibody. Images were taken with 100,000 counts collected from each mouse using the A-Spect system (Gamma Medica, Inc.), equipped with a 2-mm pinhole collimator.

Blinded diagnostic study

In order to replicate a scenario more relevant to clinical practice, an observer experiment was conducted in which the antibody cocktail was injected into mice expressing only one of the tumor types, five mice with two A431 tumors, and five mice with two 3T3/HER2+ tumors. Spectrally resolved images were sequentially shown to observers by covering over one lesion on the image producing 10 images per tumor group and 20 tumor images altogether. These images were placed in random order and shown to two investigators, experienced in optical imaging, who were aware of the variables used for the initial experiments (Y. Hama and H. Kobayashi) but who were blinded to the tumor types present in each mouse. The investigators were asked to correctly identify the correct tumor type based on the fluorescence pattern of each tumor. Thus, a total of 40 images were submitted for assessment by two observers.

Results

In vitro analysis

Flow cytometry study. Fluorescence-activated cell sorting studies showed appropriate binding of each antibody conjugate to the cell line expressing the respective characteristic antigen (Fig. 2A-B). Cetuximab-RhodG showed strong binding affinity to the HER1-overexpressing A431 cells, as shown by the mean fluorescence index, which is several orders of magnitude higher (10^3) than control cells. Incubation of A431 cells with trastuzumab-RhodG produced slightly higher binding than

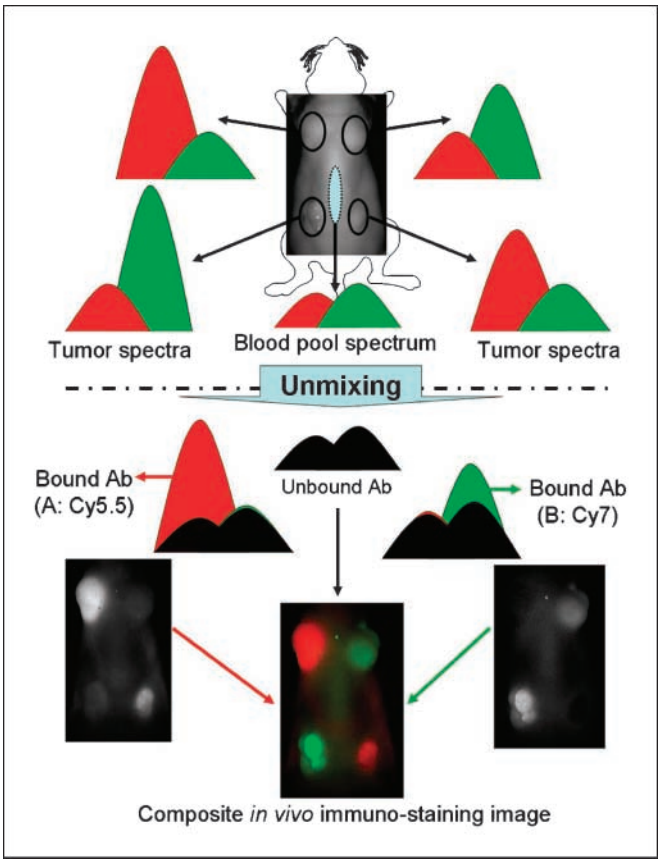

Fig. 1. Schema representing the acquisition and post-processing of optical images on the CRi Maestro In-Vivo Imaging System (see Supplemental Fig. S1 for respective tumor locations). Spectral fluorescence images consisting of blood pool, Cy5.5, and Cy7 spectra were obtained. Spectral libraries for Cy5.5 and Cy7 were imported and the respective spectra unmixed to produce a composite image.

control cells, indicating either minimal specific binding of the antibody or nonspecific binding (Fig. 2A). Trastuzumab-RhodG showed high affinity for the 3T3 cells engineered to express HER2 receptors. Incubation with cetuximab-RhodG again showed low levels of binding to 3T3 HER2+ cells compared with control cells, which is likely representative of nonspecific binding in this non–HER1 receptor–expressing cell line (Fig. 2B).

Fluorescence microscopy. Fluorescence microscopy was used to show the binding of fluorescently-labeled antibody to cells *in vitro*. Cetuximab-Cy5.5 bound to the surface of A431 cells as early as 1 h postincubation (Fig. 2C). The antibody conjugate was gradually internalized, and became perinuclear 24 h post-incubation. Trastuzumab-Cy7 also bound to the surface of 3T3/HER2+ cells within 1 h after incubation, with the complex gradually internalizing over the next several hours (Fig. 2C). Control experiments showed no binding of either trastuzumab-Cy7 to A431 cells, or cetuximab-Cy5.5 to 3T3/HER2+ cells (Fig. 2C).

Immunoreactivity and receptor numbers. Specific binding of antibody was found only for ^{111}In labeled cetuximab against A431 cells and ^{111}In-labeled trastuzumab against 3T3/HER2+ cells. Receptor number on each cell was calculated using the Scatchard plot analysis (14), and was found to be ~1.5 million copies of HER1 for A431 cells, and ~2.2 million copies of HER2 for 3T3/HER2+ cells. These figures are consistent with previously reported numbers for receptor overexpression (15).

In vivo imaging

Spectral fluorescence imaging following injection of an antibody cocktail can distinguish tumors that overexpress either HER1 or HER2 receptors. Initial experiments showed clear differentiation on spectral images between the two tumor types A431 and 3T3/HER2+ after administration of the antibody-optical agent cocktail of cetuximab-Cy5.5 and trastuzumab-Cy7 (Fig. 3). Tumor growth rates were variable, and to ensure optimal imaging conditions, further experiments were monitored 10 to 14 days postimplantation for tumor growth, and imaging was undertaken when appropriate tumor sizes were reached. The optimal antibody dose was determined to be 50 μg for both cetuximab and trastuzumab, and the best imaging time was shown to be 24 h after injection of the antibody cocktail. Following the initial proof of principle experiments, subsequent experiments employed Balb3T3/DsRed tumors as a control. The latter tumor serves as a control because it expresses neither HER1 nor HER2 receptors, but has been engineered to express red fluorescence protein. Thus, there should be only minimal (blood pool) uptake of the antibody-optical agents, but the presence of tumor could be shown by imaging in the green light range and detecting the inherent red fluorescence.

Further control experiments were also established as follows (data not included). Two mice were imaged after tumors reached an appropriate size, without administration of the antibody cocktail; no enhancement was seen on either Cy5.5 or Cy7 spectra. Additionally, crossover antibody experiments were undertaken, wherein a cocktail of cetuximab linked to Cy7 and trastuzumab linked to Cy5.5 was prepared. Two mice showed appropriate uptake of the agents, with 3T3/HER2+ tumors having appropriate peaks in the Cy5.5 spectra range, and A431 tumors expressing peaks in the Cy7 spectra.

Radionuclide imaging can diagnose the distinct tumor types, but takes longer than spectral fluorescence imaging. Scintigraphy revealed that the two radiolabeled antibodies showed different biodistribution and tumor accumulation patterns. Cetuximab was quickly cleared from the circulation and accumulated in the liver within 24 h, thus cetuximab produced a better tumor-to-background ratio for A431 tumors as well as a better A431 tumor-to-3T3/HER2+ tumor ratio (Fig. 4A). In contrast, trastuzumab was cleared from the circulation much more slowly than cetuximab. Therefore, prolonged high background activity derived from the retention of the agent in the blood pool compromised the 3T3/HER2+ tumor-to-background ratio as well as 3T3/HER2+ tumor-to-A431 tumor ratio (Fig. 4B). Therefore, specific accumulation of trastuzumab into 3T3/HER2+ was not apparent until at least 2 days postinjection, but was visualized most clearly at 4 days after injection—when the blood activity went down.

In all 14 mice, spectral fluorescence imaging was able to differentiate A431, 3T3/HER2+, and Balb3T3/DsRed 24 h after injection of the antibody cocktail both *in vivo* (Fig. 4C) and *ex vivo*, post-resection (Fig. 4D). However, A431 tumors were clearer, implying increased uptake of its respective antibody-optical agent conjugate. As expected, the Balb3T3/DsRed tumors produced spectra consistent with a mixture of the two optical agents. This can be explained by the combined presence of both optically labeled antibodies within the blood pool in

the tumor. Using spectrally resolved optical imaging, the background signal can be subtracted, thus producing an earlier and clearer differentiation of tumor subtype, when compared with scintigraphic techniques.

Cocktail injection of two specific antibodies can distinguish the expression of EGFRs, even when only one tumor exists in the body. Having established the ability of the technique to differentiate two different tumors simultaneously *in vivo*, we also attempted to replicate another clinical scenario in which only one tumor subtype was present. Ten additional mice implanted with either A431 or 3T3/HER2+ were imaged after injection of the optically labeled antibody cocktail (Supplemental Table S1) and the images were presented to two authors (H. Kobayashi and Y. Hama) who were blinded to the tumor type (example images are provided in Supplemental Fig. S2). Both investigators were individually able to correctly diagnose tumors in all of their 20 cases, giving a total accuracy of 100% (40/40 cases).

In order to quantify these results, pixel intensity values were obtained from both the Cy5.5 and Cy7 spectral images for each tumor. Regions of interest were drawn around each of the two tumors and the midline region (to measure the background signal; Fig. 5A-B). Average pixel intensities from the regions of interest in the tumor were divided by the average pixel intensity from the background regions of interest to derive a signal-to-noise ratio. The process was repeated for each tumor using Cy5.5 spectral and Cy7 spectral images using the same regions of interest (Table 1). It was expected that because 3T3/HER2+ tumors bind trastuzumab-Cy7, they would have a high signal-to-noise ratio for Cy7 spectra, and a low ratio (close to background) for the Cy5.5 spectra. The opposite should be true for A431 tumors, which preferentially bind cetuximab-Cy5.5, although there was also a small amount of expression of HER2 receptors in these tumors resulting in some signal on the Cy7 spectral images. The results from Table 1 can be expressed in a scatter graph (Fig. 5C). It is clear from this graph that the two tumor types can be quantitatively differentiated, although, as expected, A431 tumors also tend to have a higher relative signal in the Cy7 spectra than 3T3/HER2+ tumors have for the Cy5.5 spectra.

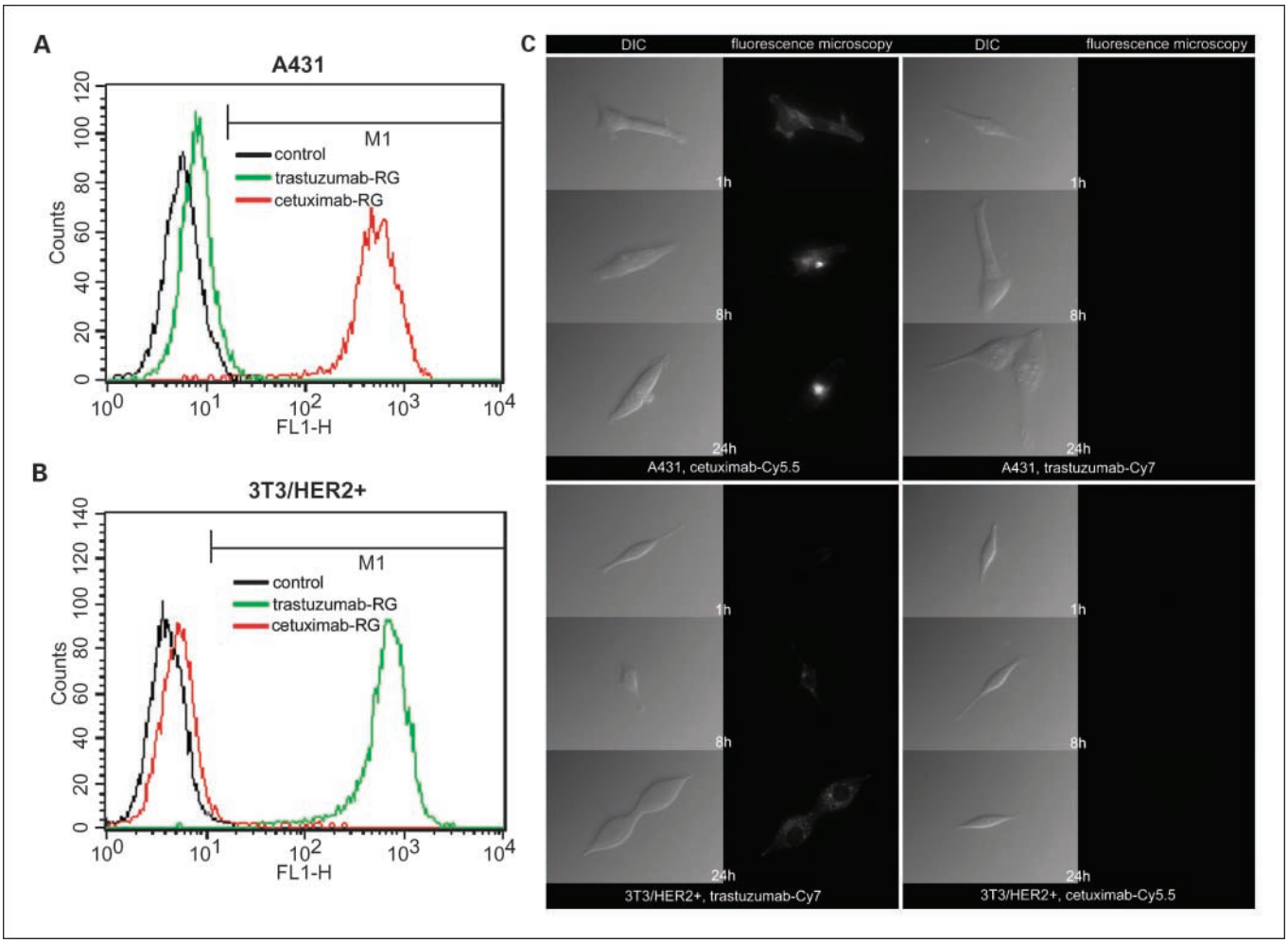

Fig. 2. Fluorescence-activated cell sorting flow cytometry and fluorescence microscopy studies. Results for A431 (*A*) and 3T3/HER2+ (*B*) cell lines 3 h after incubation with antibody linked to a fluorescent dye. Cetuximab (antibody to HER1) linked to RhodG (Erb-RG) shows strong binding affinity to HER1-overexpressing A431 cells. Trastuzumab (antibody to HER2) linked to RhodG (Herceptin-RG) shows high affinity for 3T3 cells engineered to express HER2 receptors. Note nonspecific binding of Erb-RG to 3T3/HER2+ cells not expressing HER1 receptors as compared with control cells, and nonspecific binding and/or weak binding of trastuzumab (Herceptin)-RhodG to A431 cells which minimally express HER2 receptors. *C,* microscopic studies done on Olympus BX61 microscope (magnification, ×20). A431 cells (1×10^4) incubated with cetuximab-Cy5.5 and viewed under fluorescence filter after 1, 8, and 24 h of incubation (*top left*). 3T3/HER2+ cells (1×10^4) incubated with trastuzumab-Cy7, viewed at 1, 8, and 24 h postincubation (*bottom left*). Crossover antibody control experiments show no antibody uptake (*top* and *bottom right*).

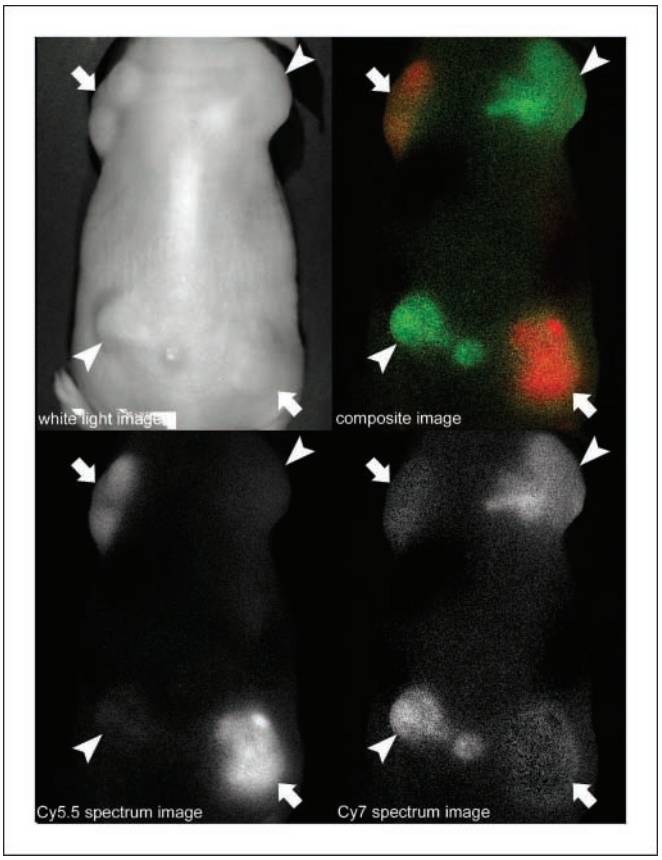

Fig. 3. *In vivo* optical imaging of two tumor types. Example from the initial proof of principle experiments, using two tumor types: A431 (*arrows*) and 3T3/HER2+ (*arrowheads*). The two tumor types have different peak wavelengths as reflected in the Cy5.5 and Cy7 spectral images; this can be unmixed on the composite image. This allows the differentiation of the two tumors types from each other and background signal, due to targeted uptake of the respective optical agent-antibody complex by each tumor type.

Discussion

This study shows that it is possible to inject a cocktail of two distinct optically labeled monoclonal antibodies and correctly identify and characterize two different tumor types, each predominantly expressing a different cell surface antigen. Initial *in vitro* experiments established binding of the antibody conjugates to their respective cell lines. Fluorescence-activated cell sorting studies showed a ~2.5-log increase in binding of cetuximab to A431 expressing HER1 receptors, and trastuzumab to 3T3/HER2+ cells expressing HER2 receptors; this was validated by the binding assay using ^{111}In-labeled antibodies. Fluorescence microscopy showed binding of the antibody complexes to the cell surface and gradual internalization into the cell. In single antibody scintigraphy studies, ^{111}In-labeled trastuzumab failed to detect specific tumor (3T3/HER2+) at 24 h and longer imaging times were required because of its prolonged serum clearance (Fig. 4A-B). However, we were able to show targeted optical imaging of two tumor subtypes *in vivo* 24 h postinjection of the antibody cocktail using optical imaging because it was possible to subtract the blood pool spectra of these NIR dyes from the tumor spectra, something that is not possible to do with radiolabeled imaging (Fig. 4C). Therefore, after optically labeled monoclonal antibodies have bound to their target, spectrally resolved imaging with background unmixing allows the correct tumor to be identified. We also replicated another clinical scenario in which only one tumor type was present. Following injection of the optically labeled antibody cocktail, observers blinded to the nature of the tumor correctly characterized all 40 of 40 tumors.

Alternative tumor models. Our experiments were used as a proof of principle of the targeted imaging technique *in vivo*, thus selection of a more simplistic model was appropriate. In order to prove that the technique is not only applicable to the cell lines we selected, we briefly carried out additional experiments on five mice, s.c. implanted with separate tumors known to overexpress HER2: the ovarian cancer cell line SKOV-3 (ref. 16; Supplemental Fig. S3). The mice were also implanted with A431 tumors to allow direct comparison. Once again, the tumors could easily be separated and subtyped following unmixing by spectral resolution (Supplemental Fig. S4).

Orthotropic implantations would provide us with a more accurate clinical model (17). In order to evaluate an orthotropic model, we conducted additional experiments in which five mice were implanted with MDA-MB-468 (by intramammary injection). MDA-MB-468 is a human breast adenocarcinoma cell line that overexpresses HER1, but has only a minimal expression of HER2 (refs. 18, 19; Supplemental Fig. S3). These mice were also s.c. implanted with the HER2-positive gastric carcinoma cell line N87 (Supplemental Fig. S3) or ovarian cancer cell line SKOV-3 periumbilically for comparison. Once again, the two tumor types could be successfully differentiated after spectral unmixing (Supplemental Figs. S5 and S6), proving that orthotropic models could also be studied using our techniques. Furthermore, genetically engineered spontaneous cancer models are the most optimal way to study tumors. Herein, different spontaneous tumor cell lines could be engineered to express a different colored fluorescent protein, along with a specific receptor overexpression (20). Subsequently, targeted optical-antibody imaging could be correlated to the "auto"-fluorescence produced by the fluorescence proteins within the tumor cells, detected at different optical wavelengths. Such techniques might prove to be a useful means of testing its ability to quantify receptor expression in mixed overexpression models. We did not study this directly and this would be an area for further work, however, we did use a red fluorescence protein–transfected cell line as a control (Balb3T3/DsRed), thus establishing the ability of our technique to detect inherent fluorescence expression.

It could be contended that, in some clinical circumstances, tumors may overexpress one, two, or more receptor targets to varying degrees, and the use of models in which only one receptor is highly overexpressed is not representative of this. Nevertheless, the technique needs to be established before it can be refined, and further tested for the ability to detect smaller copies of targets and to quantify the extent of overexpression in mixed models.

Clinical implications. This work has a number of practical implications. From the perspective of whole-body imaging, only positron emission tomography and a single photon emission computed tomography have sufficient coverage and sensitivity for targeted imaging of HER1 and HER2 receptors *in vivo* (21). However, positron emission tomography and single photon emission computed tomography are limited in their spatial resolution, expose the patient to ionizing radiation

and, because they are monochromatic, only one type of signal is generated, limiting the ability to differentiate more than one target at a time. In contrast, optical imaging not only has high sensitivity and good temporospatial resolution but is also polychromatic, opening up the possibility for multicolor, multiparameter imaging. However, it is limited in its ability to penetrate tissue deep to the surface. The use of NIR fluorescence and improvements in instrumentation may help to overcome this limitation but optical imaging is still fundamentally limited to surface targets. More realistically, optical imaging can be envisioned to detect superficial tumors (i.e., breast), or it can be adapted for endoscopic or surgical use (e.g., esophageal-gastro-duodenoscopy, bronchoscopy, colonoscopy, laparoscopic surgery). Furthermore, its ease of use, real-time acquisition and lower cost compared with positron emission tomography and single photon emission computed tomography, make optical imaging an ideal modality for intraoperative or endoscopic imaging.

Clinical relevance. The EGFRs HER1 and HER2 were used as targets in this study. As previously noted these receptors are found on a number of tumor types, including ovarian, breast, and lung cancer although they are not always overexpressed (4, 5); additionally, they can be found on normal epithelial tissue but at much lower levels of expression (22, 23). We used

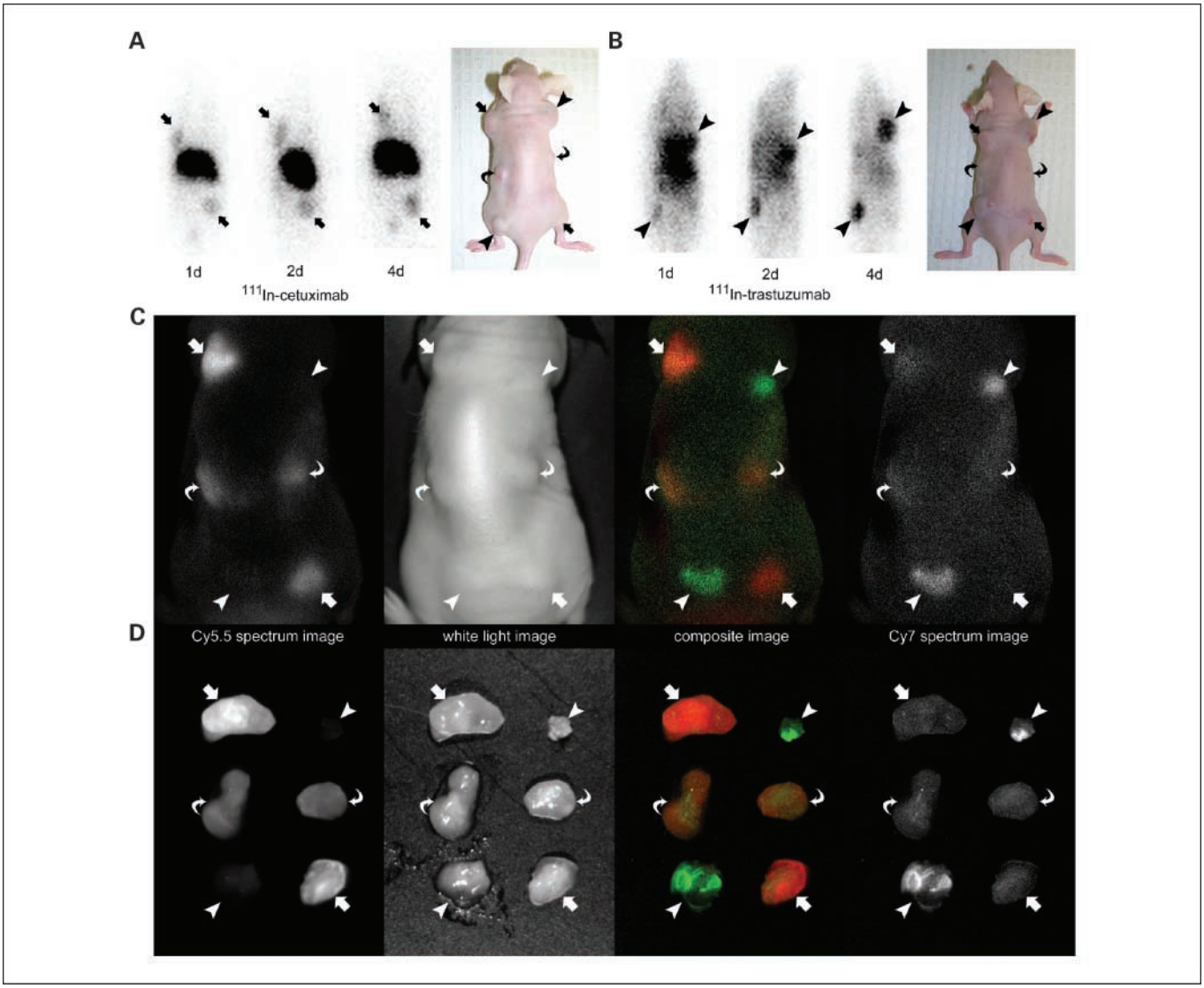

Fig. 4. ^{111}In scintigraphy experiments and multitumor *in vivo* spectral fluorescence compared. Fifty micrograms of ^{111}In-labeled cetuximab (*A*) or trastuzumab (*B*) injected into mice bearing A431 (*arrows*), 3T3/HER2+ (*arrowheads*), and Balb3T3/DsRed tumors. Serial scintigrams were taken at 1, 2, and 4 d after injection. Tumor locations are shown. Cetuximab is quickly cleared from the circulation, being seen predominantly in the liver and A431 tumors as early as 1 d. Trastuzumab is cleared from the circulation more gradually, producing a prolonged high background; specific accumulation into the 3T3/HER2+ tumors is not apparent until at least 2 days, but most clearly at 4 d, after injection, when the blood activity goes down. *In vivo* (*C*) and *ex vivo* (*D*) optical imaging from mouse 13. Curved arrow, Balb3T3/DsRed tumors. *C,* white light images show tumor location. Cy5.5 spectral image shows strong uptake of cetuximab-Cy5.5 by A431 tumors, presence in the blood pool of the agent from Balb3T3/DsRed tumors, and no uptake by 3T3/HER2+ tumors. Cy7 spectral image shows increased uptake of trastuzumab-Cy7 by 3T3/HER2+ tumors, and low presence associated with Balb3T3/DsRed (likely blood pool uptake) and A431 (possibly weak binding, or blood pool uptake). The composite image (unmixing) allows the differentiation of the tumors: red, A431; green, 3T3/HER2+; orange (mixed color), Balb3T3/DsRed. *D, ex vivo* images reflect the *in vivo* findings. Removal of background signal more clearly shows the presence of a mixture of antibody-optical agents in the Balb3T3/DsRed tumors.

the antibodies cetuximab (erbitux) and trastuzumab (herceptin), both FDA-approved monoclonal antibodies, to target the receptors HER1 and HER2, respectively. These antibodies are clinically relevant: herceptin is FDA-approved for the treatment of HER2-overexpressing, lymph node–positive breast cancer (24). Erbitux is FDA-approved for the treatment of patients with advanced metastatic colorectal cancer and, in combination with radiation therapy, for patients with squamous cell cancer of the head and neck that cannot be removed by surgery (25).

Advantages over radionuclide imaging. A characteristic of monoclonal antibodies is that they clear very slowly from the blood pool, leaving a background signal, making target detection more difficult. This is unavoidable with radionuclide imaging because there is no way of reducing background signal without also reducing the target signal but can be substantially reduced with spectral unmixing using optical imaging. Even so, unmixing is not a perfect solution. The problem of background signal was highlighted by the observation that A431 tumors produced a small, but noticeable signal in the Cy7 range (fluorescent dye linked to the HER2-selective trastuzumab) and 3T3/HER2+ tumors produced a small amount of signal in the Cy5.5 range (dye linked to the HER1-selective cetuximab). In the case of the weakly HER2-expressing A431 tumors, this could represent minimal binding of the trastuzumab-Cy7 to the tumor. However, 3T3/HER2+ tumors do not express HER1 receptors, thus, any signal corresponding to the Cy5.5 spectra represents background blood pool signals from the cetuximab-Cy5.5 complex. Tumors have an increased blood volume compared with normal tissue and nonspecific accumulation of unbound antibody conjugate within or near the tumor is a real possibility, and might affect the specificity of detection with these agents. This finding is consistent with the tumor accumulation shown by scintigraphy, from which it is not possible to subtract the blood pool because of the monochromatic nature of radionuclide imaging. In theory, using different radioisotopes with different energies, it might be possible to

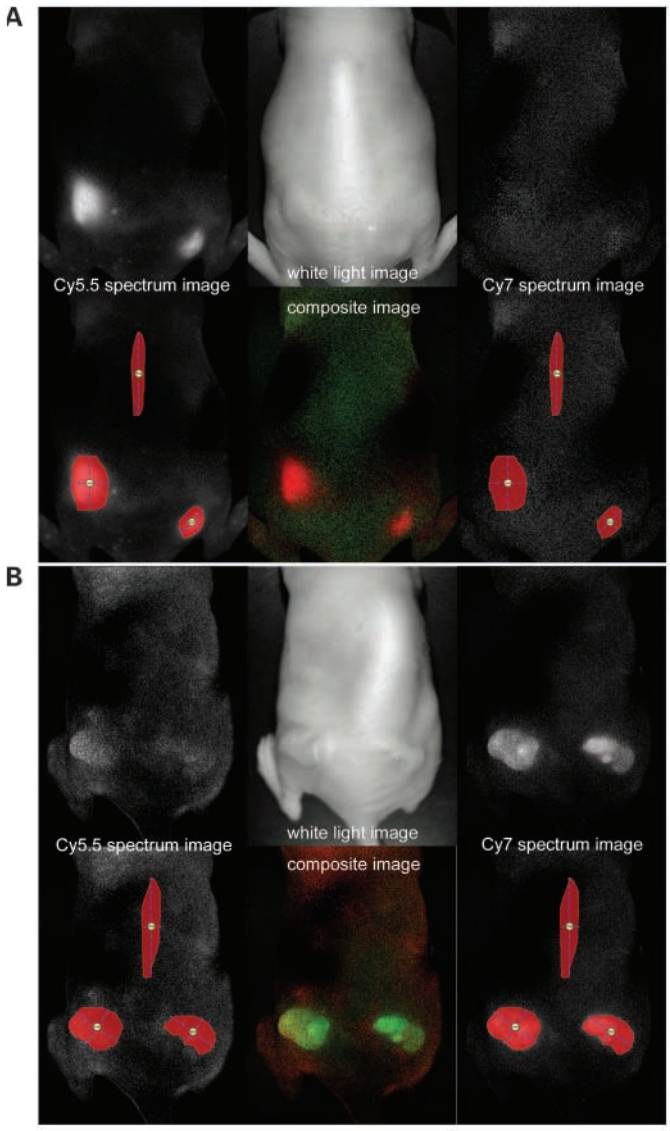

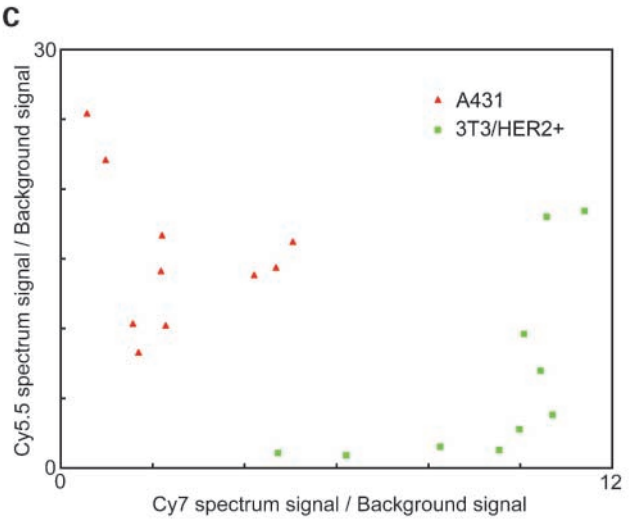

Fig. 5. Quantification of antibody uptake in blinded diagnostic study. Example of mice bearing either A431 (*A*) or 3T3/HER2+ (*B*) tumors. Regions of interest are drawn around the two tumors (left and right flanks) and midline (for background signal). Pixel intensity values are derived from both Cy5.5 and Cy7 spectra, enabling signal-to-noise ratios to be derived for the two tumor subtypes in each spectral range. See Table 1 for full list of quantitative results. *C,* scatter graph showing quantitative ratios derived from A431 (*red*) and 3T3/HER2+ (*green*) tumors in both Cy5.5 and Cy7 spectra. This allows the two tumor types to be clearly differentiated.

Table 1. Quantitative values of pixel intensity per tumor in the Cy5.5 and Cy7 spectral range

Mouse	Regions of interest, average pixel intensity						Signal-to-noise ratios	
	Tumor subtype	Tumor location	Tumor Cy5.5	Tumor Cy7	Midline Cy5.5	Midline Cy7	Tumor/BG (Cy5.5)	Tumor/BG (Cy7)
1	3T3/HER2+	Right flank	111.27	46.25	29.27	4.32	3.80	10.71
1	3T3/HER2+	Left flank	81.33	43.13	29.27	4.32	2.78	9.98
2	3T3/HER2+	Right flank	46.49	24.51	43.10	5.18	1.08	4.73
2	3T3/HER2+	Left flank	38.86	32.17	43.10	5.18	0.90	6.21
3	3T3/HER2+	Right flank	83.45	35.68	55.73	4.32	1.51	8.26
3	3T3/HER2+	Left flank	71.31	41.22	55.73	4.32	1.28	9.54
4	3T3/HER2+	Right flank	305.80	58.71	16.98	5.55	18.01	10.58
4	3T3/HER2+	Left flank	312.84	63.28	16.98	5.55	18.42	11.4
5	3T3/HER2+	Right flank	96.47	42.18	13.84	4.04	6.97	10.44
5	3T3/HER2+	Left flank	132.84	40.74	13.84	4.04	9.60	10.08
6	A431	Right flank	349.95	5.03	15.83	5.14	22.11	0.98
6	A431	Left flank	402.57	2.93	15.83	5.14	25.43	0.57
7	A431	Right flank	404.92	12.45	24.28	5.65	16.68	2.20
7	A431	Left flank	251.5	8.85	24.28	5.65	10.36	1.57
8	A431	Right flank	224.78	9.8	27.11	5.80	8.29	1.69
8	A431	Left flank	439.71	29.28	27.11	5.80	16.22	5.05
9	A431	Right flank	410.81	27.69	29.68	6.58	13.84	4.21
9	A431	Left flank	426.39	30.83	29.68	6.58	14.37	4.69
10	A431	Right flank	350.24	12.09	24.80	5.54	14.12	2.18
10	A431	Left flank	253.39	12.64	24.80	5.54	10.22	2.28

NOTE: Background values were also obtained to allow the derivation of signal-to-noise ratios.

distinguish two or more targets, however, the combined use of ionizing radiation is unappealing. In contrast, by employing additional antibodies conjugated with distinct NIR fluorophores in the cocktail, this method has a potential to distinguish two, or more (Supplement Fig. S7), receptors/antigens simultaneously, which is practically impossible to achieve with radionuclide imaging. Although quantitation would seem to be a clear advantage of radionuclide imaging, it was possible to semiquantitate the optical signal produced in the Cy5.5 and Cy7 spectra after background (blood pool) subtraction (Fig. 5; Table 1).

In conclusion, an *in vivo* NIR spectrally resolved fluorescence imaging technique is presented in which a cocktail of optically labeled antibodies, each labeled with a specific fluorophore, is injected and binds to its respective tumor. This method enables the simultaneous detection and differentiation of two distinct tumors predominantly expressing two different subtypes of EGFR: HER1 and HER2. Because spectrally resolved optical imaging has the potential to subtract both autofluorescence as well as the "blood pool" background and depict the specific accumulation of antibody within the target tumor, the technique can be adapted to give semiquantitative results on the basis of pixel intensity in a given spectral peak. Furthermore, it is possible for observers to accurately recognize the targeting of optical agents to specific receptors by simply viewing the images. Thus, this technique could potentially be adapted for clinical applications, such as aiding endoscopic and surgical procedures.

References

1. Maihle NJ, Baron AT, Barrette BA, et al. EGF/ErbB receptor family in ovarian cancer. Cancer Treat Res 2002;107:247–58.
2. YamamotoT, Ikawa S, AkiyamaT, et al. Similarity of protein encoded by the human c-erb-B-2 gene to epidermal growth factor receptor. Nature 1986;319:230–4.
3. Prenzel N, Fischer OM, Streit S, Hart S, Ullrich A. The epidermal growth factor receptor family as a central element for cellular signal transduction and diversification. Endocr Relat Cancer 2001;8:11–31.
4. Gullick WJ, Marsden JJ, Whittle N, Ward B, Bobrow L, Waterfield MD. Expression of epidermal growth factor receptors on human cervical, ovarian, and vulval carcinomas. Cancer Res 1986;46:285–92.
5. Salomon DS, Brandt R, Ciardiello F, Normanno N. Epidermal growth factor-related peptides and their receptors in human malignancies. Crit Rev Oncol Hematol 1995;19:183–232.
6. Souder C, Leitzel K, Ali SM, et al. Serum epidermal growth factor receptor/HER-2 predicts poor survival in patients with metastatic breast cancer. Cancer 2006;107:2337–45.
7. Carrington C. Optical imaging sheds light on cancer's signature—regional blood flow and tissue oxygenization measures may permit earlier breast cancer detection. Diagnostic Imaging 2004, June. Available from: http://www.diagnosticimaging.com/molecularimagingoutlook/2004jun/.
8. Di Fiore PP, Pierce JH, Kraus MH, Segatto O, King CR, Aaronson SA. erbB-2 is a potent oncogene when overexpressed in NIH/3T3 cells. Science 1987;237:178–82.
9. Kobayashi H, Wu C, Yoo TM, et al. Evaluation of the *in vivo* biodistribution of yttrium-labeled isomers of CHX-DTPA-conjugated monoclonal antibodies. J Nucl Med 1998;39:829–36.
10. Wu C, Kobayashi H, Sun B, et al. Stereochemical influence on the stability of radio-metal complexes *in vivo*. Synthesis and evaluation of the four stereoisomers of 2-(p-nitrobenzyl)-trans-CyDTPA. Bioorg Med Chem 1997;5:1925–34.
11. Camera L, Kinuya S, Garmestani K, et al. Evaluation of a new DTPA-derivative chelator: comparative biodistribution and imaging studies of 111In-labeled B3 monoclonal antibody in athymic mice bearing human epidermoid carcinoma xenografts. Nucl Med Biol 1993;20:955–62.
12. Kobayashi H, Yoo TM, Kim IS, et al. L-lysine effectively blocks renal uptake of ^{125}I- or ^{99m}Tc-labeled anti-Tac dsFv. Cancer Res 1996;56:3788–95.
13. Kobayashi H, Sakahara H, Saga T, et al. A human/mouse chimeric monoclonal antibody against CA125 for radioimmunoimaging of ovarian cancer. Cancer Immunol Immunother 1993;37:143–9.
14. LindmoT, Boven E, Cuttitta F, Fedorko J, Bunn PA, Jr. Determination of the immunoreactive fraction of radiolabeled monoclonal antibodies by linear extrapolation to binding at infinite antigen excess. J Immunol Methods 1984;72:77–89.
15. Krupp MN, Connolly DT, Lane MD. Synthesis, turnover, and down-regulation of epidermal growth factor receptors in human A431 epidermoid carcinoma cells and skin fibroblasts. J Biol Chem 1982;257:11489–96.
16. Clinchy B, Gazdar A, Rabinovsky R, Yefenof E, Gordon B, Vitetta ES. The growth and metastasis of human, HER-2/neu-overexpressing tumor cell lines in

male SCID mice. Breast Cancer Res Treat 2000;61:217–28.

17. Hoffman RM. Orthotopic metastatic mouse models for anticancer drug discovery and evaluation: a bridge to the clinic. Invest New Drugs 1999;17:343–59.

18. Konecny GE, Pegram MD, Venkatesan N, et al. Activity of the dual kinase inhibitor lapatinib (GW572016) against HER-2-overexpressing and trastuzumab-treated breast cancer cells. Cancer Res 2006;66:1630–9.

19. Biscardi JS, Belsches AP, Parsons SJ. Characterization of human epidermal growth factor receptor and c-Src interactions in human breast tumor cells. Mol Carcinog 1998;21:261–72.

20. Hoffman RM. The multiple uses of fluorescent proteins to visualize cancer *in vivo*. Nat Rev Cancer 2005;5:796–806.

21. Chatziioannou AF. Instrumentation for molecular imaging in preclinical research: Micro-PET and Micro-SPECT. Proc Am Thorac Soc 2005;2:533–6, 10–1.

22. Cohen BD, Siegall CB, Bacus S, et al. Role of epidermal growth factor receptor family members in growth and differentiation of breast carcinoma. Biochem Soc Symp 1998;63:199–210.

23. Sliwkowski MX, Schaefer G, Akita RW, et al. Coexpression of erbB2 and erbB3 proteins reconstitutes a high affinity receptor for heregulin. J Biol Chem 1994;269:14661–5.

24. Piccart-Gebhart MJ. Adjuvant trastuzumab therapy for HER2-overexpressing breast cancer: what we know and what we still need to learn. Eur J Cancer 2006;42:1715–9.

25. Available from: http://www.fda.gov/cder/drug/infopage/erbitux/default.htm.

Clinical Cancer Research

In vivo Diagnosis of Epidermal Growth Factor Receptor Expression using Molecular Imaging with a Cocktail of Optically Labeled Monoclonal Antibodies

Tristan Barrett, Yoshinori Koyama, Yukihiro Hama, et al.

Clin Cancer Res 2007;13:6639-6648.